

---

# Distributed non-disclosive validation of predictive models by a modified ROC-GLM

Daniel Schalk\*, Verena Sophia Hoffmann<sup>2,3</sup>, Bernd Bischl<sup>1</sup>, and Ulrich Mansmann<sup>1,2,3</sup>

<sup>1</sup> Department of Statistics, LMU Munich, Munich, Germany

<sup>2</sup> Institute for Medical Information Processing, Biometry and Epidemiology, LMU Munich, Munich, Germany

<sup>3</sup> DIFUTURE (DataIntegration for Future Medicine, [www.difuture.de](http://www.difuture.de)), LMU Munich, Munich, Germany

Distributed statistical analyses provide a promising approach for privacy protection when analysing data distributed over several databases. It brings the analysis to the data and not the data to the analysis. The analyst receives anonymous summary statistics which are combined to an aggregated result. We are interested to calculate the AUC of a prediction score based on a distributed approach without getting to know the data of involved individual subjects distributed over different databases. We use DataSHIELD as the technology to carry out distributed analyses and use newly developed algorithms to perform the validation of the prediction score. Calibration can easily be implemented in the distributed setting. But, discrimination represented by a respective ROC curve and its AUC is challenging. We base our approach on the ROC-GLM algorithm as well as on ideas of differential privacy. The proposed algorithms are evaluated in a simulation study. A real-world application is described: The audit use case of DIFUTURE (Medical Informatics Initiative) with the goal to validate a treatment prediction rule of patients with newly diagnosed multiple sclerosis.

*Key words:* Area under the ROC curve; Distributed computing; Medical tests; ROC-GLM;

## 1 Introduction

Medical research is based on the trust that the analysis of confidential patient data follows principles of privacy protection. However, depending on the released data and proposed diagnosis, breaches to the patient's privacy may occur (Loukides et al., 2010). Even when a patient gives an informed consent, that the researcher can have access to his/her pseudomized patient data, it is necessary to keep data in a protected environment and to process it accordingly. As described by Arellano et al. (2018), when the protection of sensitive patient data is a key objective, privacy-preserving predictive modelling should be considered. Typically, multi-center studies in medicine or epidemiology collect the data in a central study database and perform the analyses in a specifically protected environment following the informed consent of the study subjects. Analogously, in big-data real world applications the data of interest may be provided by different locations and may be transferred from there to a central database for analysis. But, this requires an administratively challenging and time-consuming trustful data sharing process.

The administrative load for data sharing is alleviated if the researcher only uses anonymous and aggregated data for his analysis. Therefore, the new concept of distributed data network studies allows to leverage routinely collected electronic health data by reducing the administrative work of the conventional

---

\*Corresponding author: e-mail: [daniel.schalk@stat.uni-muenchen.de](mailto:daniel.schalk@stat.uni-muenchen.de)<sup>1,3</sup>

data sharing. Non-disclosing distributed analysis is an important part of this concept that enables statistical analyses without sharing individual patient data (IPD) between the various sites of a clinical study or sharing IPD with a central analysis-unit. Thus, non-disclosing distributed analyses protect privacy and enhance data security. Therefore, methods are needed to support robust multivariable-adjusted statistical analysis without the need to centralize IPD, thereby providing better protection for patient privacy and confidentiality in multi-database studies.

As a part of the German Medical Informatics Initiative (MII, [www.medizininformatik-initiative.de](http://www.medizininformatik-initiative.de)) the Data Integration for Future Medicine (DIFUTURE) consortium (Prasser et al., 2018) is interested to perform distributed data network studies and provides tools as well as algorithms for non-disclosing distributed analyses. DIFUTURE's specific interest consists in the validation of a treatment decision score (TDS) for patients with newly diagnosed multiple sclerosis (MS). This use case is described in more detail in Section 6 of this paper. It is of interest to validate the calibration and discrimination of the TDS using multi-center cohort data prospectively collected at five sites by a non-disclosing distributed analysis.

The current state-of-the-art of prognostic/predictive validation in a binary classification setting is to calculate the receiver operator characteristic (ROC) curve and its area under the curve (AUC) in the pooled data as well as assessing the quality of calibration (Van Calster et al., 2019). In general, IPD transfer requires specific patient consent and data protection laws apply. Here, we present a non-disclosing distributed ROC-GLM which we use to calculate the ROC curve, its AUC and the respective confidence intervals (CIs). These methods and their implementation in DataSHIELD framework (Gaye et al., 2014) allow analyses where IPD does not leave its secured environment. This way only noisy IPD or anonymous and aggregated statistics are shared which do not allow identification of individual data. It is also shown that assessing calibration of the TDS is a straightforward task. Thus, non-disclosing distributed validation of prediction and prognostic tools is a milestone in data-driven medicine and can unlock a plethora of medical information for research.

**Contribution** In this paper, we describe a novel technique to calculate the ROC-GLM (Pepe, 2000) in a distributed and privacy-preserving fashion and hence conduct distributed ROC analysis. As described in Section 3.4, the ROC-GLM consists of different stages which must be adjusted to suite our privacy requests. The major contribution is to describe how these adjustments are incorporated into the ROC-GLM by using (1) differential privacy (Dwork, 2006) to obtain a privacy-preserving survivor function that can be communicated without the threat of privacy breaches and (2) secure aggregations to conduct a distributed Fisher scoring algorithm (Jones et al., 2013) to obtain parameter estimates for the ROC-GLM. Besides the ROC analysis to assess the discrimination of a classifier, we describe how the calibration can also be analysed in a distributed and privacy-preserving fashion using secure aggregations. Hence, as a minor contribution, (3) a distributed version of the Brier score (Brier et al., 1950) and calibration curve (Vuk and Curk, 2006) is introduced.

To conclude our paper, we run a simulation study to get an impression of the effect of the distributed approach on the estimation accuracy when compared to the state-of-the-art methods. Furthermore, we show an use-case with an exemplary distributed ROC analysis concluding with a comparison of the results on the pooled data.

## 2 Related literature

A similar approach is followed by Boyd et al. (2015), who calculate the AUC applying differential privacy. After calculating the AUC, they derive ROC curves suited for that AUC using a symmetric binormal ROC function similar to the ROC-GLM. However, our method directly calculates the ROC curve in a distributed differential private manner, with a possible extension to multiple covariates from which we derive the

AUC via integration techniques. Furthermore, Boyd et al. (2015) do not provide the calculation of CIs. Another approach of calculating the ROC curve uses homomorphic encryption (Ünal et al., 2021). While differential privacy introduces noise and provides less accurate estimates, homomorphic encryption yields exact estimates. This technique also does not provide the calculation of CIs and the extension to multiple covariates. To our best knowledge, the calculation of CIs via homomorphic encryption is not documented in the literature as well as the extension to multiple covariates. Up to now, no efforts seems to be spent to provide a modified ROC-GLM algorithm for non-disclosing distributed analyses.

Within the ROC-GLM, we use a distributed Fisher scoring method (Jones et al., 2013) to estimate parameters of the underlying GLM. In contrast to the distributed Fisher scoring, other methods for one specific model class were developed, as similarly done for logistic regression (Wu et al., 2012) or for cox models (Lu et al., 2015). These methods gives lossless estimates but require multiple communication rounds. Although the communication rounds of the Fisher scoring is limited by the maximal number of iterations and also the amount of transferred data is (depending on the application) rather small, other techniques were developed that aim to reduce the communication costs. These one-shot algorithms estimate parameters based on homogeneous data with just one communication round (e.g., for logistic regression (Duan et al., 2020)) but lack in generalization to heterogeneous data. We would like to highlight that, for the ROC-GLM, the transferred data when using the distributed Fisher scoring is very small, and therefore, communication is no bottleneck. Hence, we cannot identify any threats when using the method proposed by Jones et al. (2013) over the other mentioned techniques for distributed calculations.

### 3 Terminology and the ROC-GLM

Throughout this paper, we restrict the use case to binary classification. The two classes are denoted with 1 for the positive class (i.e., possessing a trait of interest) and 0 for the negative class (i.e., lacking a trait of interest). Such traits that are often used within the frame of medicine could be, for example, "diseased" or "favorable". Within the context of this work, diseased or favorable correspond to the positive class (outcome 1), while non-diseased or non-favorable is synonymous with the negative class (outcome 0). Furthermore,  $f(x) \in \mathbb{R}$  is the score based on a true but unknown procedure  $f$ . This procedure is represented, for example, using a statistical or prediction model  $\hat{f} : \mathbb{R}^p \rightarrow \mathbb{R}$ ,  $\mathbf{x} \mapsto \hat{f}(\mathbf{x})$  given the feature vector  $\mathbf{x} \in \mathbb{R}^p$ . The data set used to fit  $\hat{f}$  is denoted as  $\mathcal{D} = \{(\mathbf{x}_1, y_1), \dots, (\mathbf{x}_n, y_n)\}$  with  $y_i \in \{1, 0\}$ . The score  $\hat{f}(\mathbf{x})$  is used to build a binary classifier by a thresholding rule  $\mathbb{1}(\hat{f}(\mathbf{x}) \geq c)$ , with threshold  $c \in \mathbb{R}$  to predict classes. On an observational level,  $\mathbf{x}_{1,i}$  and  $\mathbf{x}_{0,i}$  indicate the  $i$ -th positive or  $i$ -th negative observation. Accordingly, the score of the  $i$ -th positive or negative observation is denoted by  $\hat{f}(\mathbf{x}_{1,i})$  or  $\hat{f}(\mathbf{x}_{0,i})$ . The number of observations sampled from the populations 1 and 0 are denoted by  $n_1$  and  $n_0$ . The set of the positive and negative scores is denoted by  $\mathcal{F}_1 = \{\hat{f}(\mathbf{x}_{1,i}) \mid i = 1, \dots, n_1\}$  and  $\mathcal{F}_0 = \{\hat{f}(\mathbf{x}_{0,i}) \mid i = 1, \dots, n_0\}$ , with  $\mathcal{F}_{1,i} = \hat{f}(\mathbf{x}_{1,i})$  and  $\mathcal{F}_{0,i} = \hat{f}(\mathbf{x}_{0,i})$ . We denote the random variable (RV) of a random score generated in the positive population and in the negative population by  $Y_1 = f(\mathbf{X}_1)$  and  $Y_0 = f(\mathbf{X}_0)$  with random vectors  $\mathbf{X}_1$  and  $\mathbf{X}_0$ , respectively. To avoid confusion, we want to highlight, that the random variable  $Y$  is continuous and represents the score while the outcome  $y \in \{0, 1\}$  is a binary value.

#### 3.1 ROC curve and AUC

To quantify the quality of a binary classifiers we use the true positive rate (TPR) and false positive rate (FPR) with values between 0 and 1. A good binary classifier should be able to achieve a low FPR close to zero while simultaneously obtaining a high TPR close to one. Both are probability functions  $\text{TPR}(c) = P(Y_1 \geq c) \in [0; 1]$  and  $\text{FPR}(c) = P(Y_0 \geq c) \in [0; 1]$  (Pepe, 2000), depending on the used threshold  $c \in \mathbb{R}$ . These probability functions are also known as *survivor functions*  $S_1(c) = \text{TPR}(c)$  and  $S_0(c) =$

FPR( $c$ ). The ROC curve is defined as  $\text{ROC}(c) = (S_0(c), S_1(c))$ . It quantifies the discrimination between positive and negative states by score values (Zweig and Campbell, 1993). An alternative presentation of the ROC curve is  $\text{ROC}(t) = S_1(S_0^{-1}(t))$  with a probabilistic threshold  $t \in [0, 1]$ ,  $t = S_0(c)$ , and plugging  $c = S_0^{-1}(t)$  into  $S_1$ . The AUC as measure of discrimination between positive and negative class of a classifier is then defined as integral of the ROC curve  $AUC = \int_0^1 \text{ROC}(t) dt$ .

### 3.2 Empirical calculation of the ROC curve and AUC

Calculation of the empirical ROC curve uses the *empirical survivor functions*  $S_1$  and  $S_0$ . They are defined by the empirical cumulative distribution functions (ECDF)  $F_1$  and  $F_0$ :  $\hat{S}_1 = 1 - \hat{F}_1$  and  $\hat{S}_0 = 1 - \hat{F}_0$ .

Empirical TPR and FPR values are given by  $\hat{S}_1(\hat{f}(\mathbf{x}_{0,i}))$ ,  $i = 1, \dots, n_0$  and  $\hat{S}_0(\hat{f}(\mathbf{x}_{1,i}))$ ,  $i = 1, \dots, n_1$  and are represented by the sets  $\mathcal{S}_1 = \{\hat{S}_1(\hat{f}(\mathbf{x}_{0,i})) \mid i = 1, \dots, n_0\}$  and  $\mathcal{S}_0 = \{\hat{S}_0(\hat{f}(\mathbf{x}_{1,i})) \mid i = 1, \dots, n_1\}$ . They are also called *placement values*. As described by Pepe (2003), the placement values standardize a given score relative to the class distribution. Meaning that  $\hat{S}_1(z)$  describes the placement of  $z \in \mathbb{R}$  in the positive class distribution. Hence, the set  $\mathcal{S}_1$  represents the positive placement values (TPR) and  $\mathcal{S}_0$  the negative placement values (FPR).

The empirical version of the  $\text{ROC}(t)$  is a discrete function derived from placement values  $\mathcal{S}_1 \subseteq \{0, 1/n_1, \dots, (n_1 - 1)/n_1, 1\}$  and  $\mathcal{S}_0 \subseteq \{0, 1/n_0, \dots, (n_0 - 1)/n_0, 1\}$  and its empirical AUC is a sum over rectangles of width  $1/n_0$  and height  $\hat{S}_1(\hat{f}(\mathbf{x}_{0,i}))$ :

$$AUC = n_0^{-1} \sum_{i=1}^{n_0} \hat{S}_1(\hat{f}(\mathbf{x}_{0,i})). \quad (1)$$

### 3.3 CI for the empirical AUC

The approach proposed by DeLong et al. (1988) is used to calculate CIs. They determine the variability of the estimated AUC from the empirical variance ( $\widehat{\text{var}}$ ) of the placement values:

$$\widehat{\text{var}}(AUC) = \frac{\widehat{\text{var}}(\mathcal{S}_1)}{n_0} + \frac{\widehat{\text{var}}(\mathcal{S}_0)}{n_1}. \quad (2)$$

They provide a CI for the logit AUC from which the CI for the AUC can be derived by the  $\text{logit}^{-1}$  transformation:

$$\text{ci}_\alpha(\text{logit}(AUC)) = \text{logit}(AUC) \pm \Phi^{-1}\left(1 - \frac{\alpha}{2}\right) \frac{\sqrt{\widehat{\text{var}}(AUC)}}{AUC(1 - AUC)}. \quad (3)$$

The term  $\Phi^{-1}$  denotes the quantile function of the standard normal distribution. Furthermore, statistical testing can be based on the CI. For example, testing the hypothesis  $H_0 : AUC \leq a_0$  vs.  $H_1 : AUC > a_0$  with a significance level of  $\alpha$  is done by checking whether  $\text{logit}(a_0) > a$ ,  $\forall a \in \text{ci}_\alpha$  to reject  $H_0$ .

### 3.4 The ROC-GLM

The ROC-GLM makes inference for the ROC curve using an parametric approximation by GLMs. Further details such as estimation equations or asymptotic theory can be viewed in Pepe (2003).

The ROC-GLM procedure interprets the ROC curve as  $\text{ROC}_g(t) = g(\gamma h(t))$  with link function  $g : \mathbb{R} \rightarrow [0, 1]$ ,  $\eta \mapsto g(\eta)$ , coefficient vector  $\gamma \in \mathbb{R}^l$ , and covariate vector  $h : \mathbb{R} \rightarrow \mathbb{R}^l$ ,  $t \mapsto h(t) =$

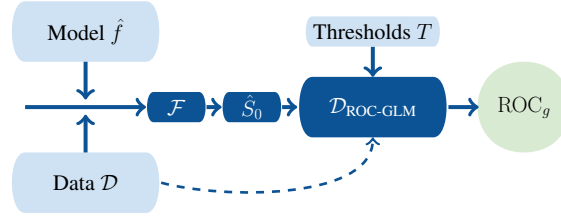


**Figure 1** All parts of the ROCGLM( $\mathcal{D}$ ) procedure, starting with the data and a model for predicting scores  $Y$ , calculating the survivor function  $\hat{S}_{\mathcal{D}}$ , and finally calculating intermediate data  $\mathcal{D}_{\text{ROC-GLM}}$  for the probit regression to obtain the parameters of the ROC-GLM  $\text{ROC}_g$ .

$(h_1(t), \dots, h_l(t))^T$ . The procedure uses the data set  $\mathcal{D}_{\text{ROC-GLM}} = \{(u_{ij}, h(t_j)) \mid i = 1, \dots, n_1, j = 1, \dots, n_T\}$  with binary response  $u_{ij} \in \{0, 1\}$  and covariates  $h(t_j)$ .

The ROC-GLM considers the binary random variable  $U_{ij} = \mathbb{1}(Y_1 \geq Y_0)$  and its expectation  $\mathbb{E}[U_{ij}] = P(Y_1 \geq Y_0) = S_1(Y_0) = S_1(S_0^{-1}(c)) = \text{ROC}(c)$ . The realisation  $u_{ij}$  of  $U_{ij}$  is calculated from placement values:  $u_{ij} = \mathbb{1}(\hat{S}_0(\mathcal{F}_{1,i}) < t_j) = \mathbb{1}(\mathcal{F}_{1,i} \geq \hat{S}_0^{-1}(t_j))$ . The additive components  $h(t)$  incorporate the thresholds  $t \in T = \{t_1, \dots, t_{n_T}\}$  into the model. The most simple ROC-GLM uses the two-dimensional vector  $h(t)$  with  $h_1(t) = 1$  and  $h_2(t) = \Phi^{-1}(t)$ . Setting the link function to  $g = \Phi$  results in a binormal form  $\text{ROC}_g(t) = \Phi(\gamma_1 + \gamma_2 \Phi^{-1}(t))$ . In this setting, the ROC-GLM is a probit regression with response variable  $u_{ij}$  covariates  $h(t_j)$ .

When calculating a ROC-GLM, one has to modify the respective data set  $\mathcal{D}$  that consists of the binary target vector  $(y_1, \dots, y_n)^T$  and the covariates  $x_i$ . Hence, based on the data  $\mathcal{D}$  the score values  $\mathcal{F}$  per patient and placement values  $S_1$  are calculated. A common choice for the thresholds is to use an equidistant grid of thresholds  $T$  to determine  $\mathcal{D}_{\text{ROC-GLM}}$  which is used to fit the ROC-GLM to estimate  $\gamma$ . In the following, we denote this estimation of  $\gamma$  on the data set  $\mathcal{D}$  as  $\text{ROCGLM}(\mathcal{D}) = \gamma$ . The AUC obtained by the ROC-GLM is the integral  $\text{AUC}_{\text{ROC-GLM}} = \int_0^1 \text{ROC}_g(t) dt$ . To calculate the AUC we use the `Rs.integrate` function that conducts a globally adaptive interval subdivision in connection with extrapolation by Wynn's Epsilon algorithm. The Gauss-Kronrod quadrature is used to get starting values. The procedure is described by Piessens et al. (2012).

## 4 Distributed ROC-GLM

### 4.1 General principles

A total of  $K$  data sets are distributed over a network of  $K$  sites:  $\mathcal{D}^{(1)}, \dots, \mathcal{D}^{(K)}$ . Each data set  $\mathcal{D}^{(k)}$  consists out of  $n^{(k)}$  observations  $(x_i^{(k)}, y_i^{(k)})$ . The  $i^{\text{th}}$  feature vector of the  $k^{\text{th}}$  site is denoted by  $x_{:,i}^{(k)}$ . The  $i^{\text{th}}$  outcome on site  $k$  is  $y_i^{(k)}$ . We assume the distributed data as part of the full but inaccessible data set:

$$\mathcal{D} = \bigcup_{k=1}^K \mathcal{D}^{(k)}, \quad n = n^{(1)} + \dots + n^{(K)} \quad (4)$$

Instead of calculating the ROC-GLM for one local data set, we want to calculate it on  $K$  distributed data sets  $\mathcal{D}^{(1)}, \dots, \mathcal{D}^{(K)}$  located at remote sites. These data are confidential and therefore it is not allowed to share parts of it. All information which are shared with the central analyst must comply with the following non-disclosing analysis principles:

**A1** Share aggregated values from which it is not possible to derive original values. Therefore, an aggregation  $a : \mathbb{R}^d \mapsto \mathbb{R}$ ,  $\mathbf{v} \rightarrow a(\mathbf{v})$  with  $d \geq q \in \mathbb{N}$  must be applied to allow sharing the value  $a(\mathbf{v})$ . The value of  $q$  is a *privacy level* guaranteeing that at least  $q$  values were used to gain  $a(\mathbf{v})$ . In the distributed setup, the values  $a(\mathbf{v}^{(k)})$  shared from each of the  $K$  sites can then be further processed. For example, calculating the mean of the  $j$ th feature vector  $\mathbf{x}_{:,j} = (\mathbf{x}_{:,j}^{(1)}, \dots, \mathbf{x}_{:,j}^{(K)})$  can be done by setting  $a(\mathbf{v}) = a_{\text{sum}}(\mathbf{v}^{(k)}) = \sum_{i=1}^{d_k} v_i^{(k)}$ ,  $\mathbf{v}^{(k)} = \mathbf{x}_{:,j}^{(k)}$ , and the respective  $d_k = n^{(k)}$ . The average is finally calculated via  $m_{\text{distr}} = n^{-1} \sum_k a_{\text{sum}}(\mathbf{x}_{:,j}^{(k)})$ . Practically, the privacy level is set prior to the analysis and stops the communication if an aggregation attempts to compute values using a  $d_k < q$ .

**A2** Use differential privacy (Dwork, 2006) to ensure non-disclosive IPD via a noisy representation. The technique we employ throughout this article is the Gaussian mechanism (Dwork et al., 2014) and is further explained in Section 4.2.

In this paper we approximate  $\text{ROCGLM}(\mathcal{D})$  by  $\text{distrROCGLM}(\mathcal{D}^{(1)}, \dots, \mathcal{D}^{(K)})$  based on the algorithm  $\text{distrROCGLM}$  that has to fulfill **A1** or **A2** to ensure privacy.

**Example: Distributed Brier score and calibration curve** Assessing probabilistic (or scoring) classifiers is often distinguished in the assessment of the discrimination and calibration. It is known that the AUC is a value to measure the discrimination. Very common methods to assess the calibration of a probabilistic classifier is to use the Brier score (Brier et al., 1950) as a quantitative measure or to plot calibration curves (Vuk and Curk, 2006) as a visual method. Both can be calculated by just depending on **A1**.

*Brier score:* The Brier score BS is defined as the mean squared error of the true 0-1-labels and the predicted probabilities:

$$\text{BS} = n^{-1} \sum_{i=1}^n \left( y_i - \hat{f}(x_i) \right)^2 \quad (5)$$

Hence, having a prediction model  $\hat{f}$  at each of the  $K$  sites, we can calculate the Brier score by:

1. Calculate the residuals  $e_i^{(k)}$  based on the true label  $y_i^{(k)}$  at site  $k$  and the predicted probabilities  $\hat{f}(\mathbf{x}_i^{(k)})$ :  $e_i^{(k)} = y_i^{(k)} - \hat{f}(\mathbf{x}_i^{(k)})$ ,  $\forall i = 1, \dots, n^{(k)}$ .
2. Calculate  $a_{\text{sum}}(\mathbf{e}^{(k)} \circ \mathbf{e}^{(k)})$ , with  $\mathbf{e}^{(k)} = (e_1^{(k)}, \dots, e_{n_k}^{(k)})^\top \in \mathbb{R}^{n_k}$  and the element-wise product  $\circ$ .
3. Send  $a_{\text{sum}}(\mathbf{e}^{(k)} \circ \mathbf{e}^{(k)})$  (if  $n_k \geq q$ ) to the host, who finally calculates  $\text{BS} = n^{-1} \sum_{k=1}^K a_{\text{sum}}(\mathbf{e}^{(k)} \circ \mathbf{e}^{(k)})$ .

*Calibration curve:* Calculating a calibration curve requires discretizing the domain  $[0, 1]$  of the probabilistic classifier  $\hat{f}$  into  $n_{\text{bin}}$  bins. A common choice for the bins is to use  $n_{\text{bin}} + 1$  equidistant points  $p_i$  from 0 to 1 to construct the  $n_{\text{bin}}$  bins  $b_l = [p_l, p_{l+1}]$  for  $l = 1, \dots, n_{\text{bin}} - 1$  and  $b_{n_{\text{bin}}} = [p_{n_{\text{bin}}}, p_{n_{\text{bin}}+1}]$  for  $l = n_{\text{bin}}$ . The calibration curve is then the set of 2-dimensional points  $p_{\text{cal},l} = (\text{pf}_l, \text{tf}_l)$ , with  $\text{tf}_l = |\mathcal{I}_l|^{-1} \sum_{i \in \mathcal{I}_l} y_i$  the true fraction of  $y_i = 1$  in bin  $b_l$  and  $\text{pf}_l = |\mathcal{I}_l|^{-1} \sum_{i \in \mathcal{I}_l} \hat{f}(\mathbf{x}_i)$  the predicted fraction for outcome 1 in  $b_l$ . The set  $\mathcal{I}_l$  describes the observations for which the prediction  $\hat{f}(\mathbf{x}_i)$  falls into bin  $b_l$ :  $\mathcal{I}_l = \{i \in \{1, \dots, n\} \mid \hat{f}(\mathbf{x}_i) \in b_l\}$ . A probabilistic classifier  $\hat{f}$  is well-calibrated if the points  $p_{\text{cal},l}$  are close to the bisector.

In the distributed setup, the points  $p_{\text{cal},l}$  are constructed by applying the distributed mean to both points for each bin at each site:

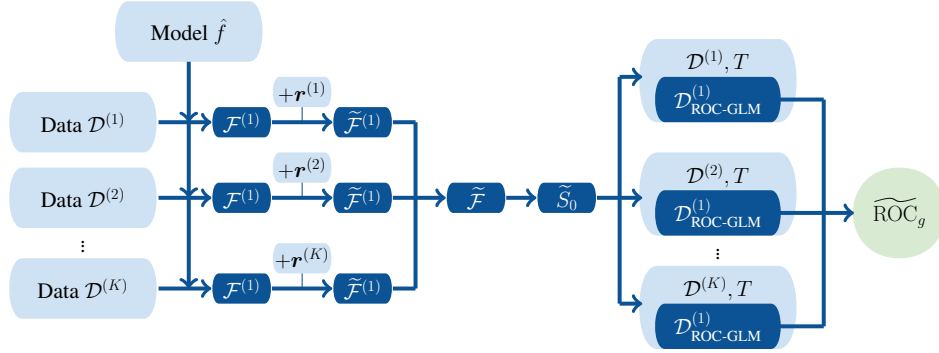


**Figure 2** All parts of the distrROCGLM procedure calculating the distributed approximation  $\widetilde{\text{ROC}}_g$  of  $\text{ROC}_g$ . The starting points are the sites (here  $K = 3$ ), which communicate scores with added noise, calculate the global survivor function  $\widetilde{S}_D$ , and finally calculate the distributed probit regression on intermediate data  $\mathcal{D}_{\text{ROC-GLM}}^{(k)}$  at each site.

1. Set all  $b_1, \dots, b_{n_{\text{bin}}}$ , and communicate them to the sites.
2. Calculate the values  $c_{l,\text{pf}}^{(k)} = a_{\text{sum}}(\{\hat{f}(\mathbf{x}_i^{(k)}) \mid i \in \mathcal{I}_l^{(k)}\})$  and  $c_{l,\text{tf}}^{(k)} = a_{\text{sum}}(\{y_i^{(k)} \mid i \in \mathcal{I}_l^{(k)}\})$  for all  $l = 1, \dots, n_{\text{bin}}$ .
3. Send  $\{(c_{l,\text{tf}}^{(k)}, c_{l,\text{pf}}^{(k)}, |\mathcal{I}_l^{(k)}|) \mid k = 1, \dots, K, l = 1, \dots, n_{\text{bin}}\}$  to the host if  $|\mathcal{I}_l^{(k)}| \geq q$ .
4. The host calculates the calibration curve  $p_{\text{cal},l}$  via  $\text{tf}_l = (\sum_{k=1}^K |\mathcal{I}_l^{(k)}|)^{-1} \sum_{k=1}^K c_{l,\text{tf}}^{(k)}$  and  $\text{pf}_l = (\sum_{k=1}^K |\mathcal{I}_l^{(k)}|)^{-1} \sum_{k=1}^K c_{l,\text{pf}}^{(k)}$  for  $l = 1, \dots, n_{\text{bin}}$ .

**Parts of the distributed ROC-GLM** The distrROCGLM is a distributed version of the ROC-GLM (see Section 3.4). Two aspects are important to construct this algorithm: First, the distributed version of the empirical survivor function; Second, a distributed version of the probit regression. Figure 2 shows the general procedure in more detail. The starting point of the distributed ROC-GLM is the private data  $\mathcal{D}^{(1)}, \dots, \mathcal{D}^{(K)}$  on the  $K$  sites.

First, the global survivor function  $\hat{S}_0$  is approximated by  $\widetilde{S}_0$  (Section 4.2) using principle **A2**. Thus,  $\widetilde{S}_0$  does not violate privacy protection concepts. The differential privacy based computation of  $\widetilde{S}_0$  by adding noise  $\mathbf{r}^{(k)}$  to the scores on each site depends on the level of privacy induced by the  $(\varepsilon, \delta)$ -differential privacy. Both parameters are further explained in the respective sections. The accuracy of the AUC as well as its CI depends on the choice of  $\varepsilon$  and  $\delta$ . Having the survivor function  $\widetilde{S}_0$  it is transmitted to each of the  $K$  sites. Knowing  $\widetilde{S}_0$  allows to calculate intermediate data  $\mathcal{D}_{\text{ROC-GLM}}^{(k)}$  (See Section 3.4). The distributed probit regression complying with principle **A1** produces the distributed ROC-GLM parameter estimates (See Section 4.3). Obtaining the parameters of the distributed ROC-GLM, denoted by  $\widetilde{\text{ROC}}_g$ , also allows to calculate the approximated AUC, denoted by  $\widetilde{\text{AUC}}_{\text{ROC-GLM}} = \int_0^1 \widetilde{\text{ROC}}_g(t) dt$ , based on the distributed approach. Finally, the CIs can be calculated based on a variance estimation which complies with principle **A1** (See Section 4.4).

## 4.2 Approximating the global survivor functions

A major challenge in calculating the distributed ROC-GLM is a privacy-preserving approach to the calculation of the survivor function. It is not allowed to directly communicate score values  $\mathcal{F}_1^{(k)}$  from the local sites to the analyst. To handle this challenge, we apply the Gaussian mechanism (Dwork et al., 2014), which adds normally distributed noise  $\mathbf{r}^{(k)}$  to the score values to ensure  $(\varepsilon, \delta)$ -differential privacy (Dwork et al., 2006a). It consists of a randomized mechanism  $\mathcal{M} : \mathcal{X} \mapsto \mathcal{Y}$  with domain  $\mathcal{X}$  (e.g.  $\mathcal{X} = \mathbb{R}^p$ ) and target domain  $\mathcal{Y}$  (e.g.  $\mathcal{Y} = \mathbb{R}$  in regression) that transforms two adjacent inputs<sup>1</sup>  $\mathbf{x}, \mathbf{x}' \in \mathcal{X}$  in the following way: For any subset of outputs  $R \subseteq \mathcal{Y}$  the property  $P(\mathcal{M}(\mathbf{x}) \in R) \leq \exp(\varepsilon)P(\mathcal{M}(\mathbf{x}') \in R) + \delta$  holds. The value of  $\varepsilon$  controls the amount of how much privacy is guaranteed. The value of  $\delta$  is the probability that  $(\varepsilon, 0)$ -differential privacy is broken (also known as  $\varepsilon$ -differential privacy and the original definition proposed in (Dwork et al., 2006b)).

The mechanism we are aiming to protect is the prediction model  $\hat{f}$  producing the scores  $\mathcal{F}_1^{(k)}$  by adding noise  $\mathbf{r}^{(k)}$  to generate noisy score values  $\tilde{\mathcal{F}}_1^{(k)} = \mathcal{F}_1^{(k)} + \mathbf{r}^{(k)}$  at each site. Therefore, the randomized mechanism in our case is  $\mathcal{M}(\mathbf{x}) = \hat{f}(\mathbf{x}) + \mathbf{r}$ . Hence, the values communicated to the host that are pooled and used for the calculation of the global survivor function are then  $\tilde{\mathcal{F}}_1^{(k)}$  and not the original score values  $\mathcal{F}_1^{(k)}$ . Using the Gaussian mechanism provides a guideline how to generate the noise to ensure  $(\varepsilon, \delta)$ -differential privacy. Therefore, each element of the noise vector  $\mathbf{r}^{(k)}$  follows a normal distribution  $\mathcal{N}(0, \tau^2)$ . The variance can be set to any value  $\tau \geq c\Delta_2(\hat{f})/\varepsilon$  with  $c^2 > 2 \ln(1.25/\delta)$ ,  $\varepsilon \in (0, 1)$ , and  $\Delta_2(\hat{f})$  the  $\ell_2$ -sensitivity of  $\hat{f}$  measured as  $\Delta_2(\hat{f}) = \max_{\text{adjacent } \mathbf{x}, \mathbf{x}'} \|\hat{f}(\mathbf{x}) - \hat{f}(\mathbf{x}')\|_2$ . In practice, we first calculate the  $\ell_2$ -sensitivity of the prediction model  $\hat{f}$  to determine possible values for  $\varepsilon$  and  $\delta$  (see Section 5.3.1). Then, we control the amount of noise added to the algorithm by choosing  $\varepsilon$  and  $\delta$  which sets the variance of the generated noise via  $\tau = c\Delta_2(\hat{f})/\varepsilon$  and  $c = \sqrt{2 \ln(1.25/\delta)}$ . Appendix A.2. contains further details and a visualization of the Gaussian mechanism.

In summary, our method to calculate an approximation of the global survivor function  $\tilde{S}_1$  of the global survivor function  $\hat{S}_1$  contains the following steps. First, we set the value of  $\varepsilon$  and  $\tau$  to generate the noise  $\mathbf{r}^{(k)}$  at each site to generate a noisy representation  $\tilde{\mathcal{F}}_1^{(k)} = \mathcal{F}_1^{(k)} + \mathbf{r}^{(k)}$  of the original score values  $\mathcal{F}_1^{(k)}$ . These noisy scores are communicated to the host and pooled to  $\tilde{\mathcal{F}}_1 = \bigcup_{k=1}^K \tilde{\mathcal{F}}_1^{(k)}$ . The pooled noisy score values are finally used to calculate an approximation  $\tilde{S}_1$  of the global survivor function. Because of ensuring  $(\varepsilon, \delta)$ -differential privacy and hence **A2**, we are allowed to share  $\tilde{S}_1$  with all sites which can now proceed with calculating the placement values and preparing the data to get passed down to the distributed probit regression which is covered in the next section.

## 4.3 Distributed GLM

Existing solutions for distributed computing – such as federated learning (McMahan et al., 2017) – are based on an iterative process of sharing and aggregating parameter values. Although this approach could also be applied to GLMs, it may lead to inexact estimates for heterogeneous data situations (Yang et al., 2021). For distributed calculation of the GLM, we use an approach described by Jones et al. (2013) and adjust the optimization algorithm of GLMs – the Fisher scoring – at its base to estimate parameters without performance loss by making use of **A1**.

As already discussed, the basis of the ROC-GLM is a probit regression (and therefore a GLM) with  $\mathbb{E}(Y | X = x) = g(x^\top \theta)$  with link function  $g$ , response variable  $Y$ , and covariates  $X$ . The Fisher scoring

<sup>1</sup> In theory, multiple ways exist to define adjacent inputs. Throughout this article, adjacent inputs are based on a histogram representation  $\tilde{\mathbf{x}} \in \mathbb{N}^p$  and  $\tilde{\mathbf{x}}' \in \mathbb{N}^p$  of two input vectors  $\mathbf{x}$  and  $\mathbf{x}'$ . The definition of adjacent inputs is then given by an equate  $\ell_1$  norm of  $\tilde{\mathbf{x}}$  and  $\tilde{\mathbf{x}}'$  to one: adjacent  $\mathbf{x}, \mathbf{x}' \Leftrightarrow \|\tilde{\mathbf{x}} - \tilde{\mathbf{x}}'\|_1 = 1$  (see Dwork et al., 2014).



is an iterative descending technique  $\hat{\theta}_{m+1} = \hat{\theta}_m + \mathcal{I}^{-1}(\hat{\theta}_m)\mathcal{V}(\hat{\theta}_m)$  that uses second order gradient information. The components are the score vector  $\mathcal{V}(\hat{\theta}_m) = [\partial\ell_\theta(y, x)/\partial\theta]_{\theta=\hat{\theta}_m} \in \mathbb{R}^p$  and the observed Fisher information  $\mathcal{I}(\hat{\theta}_m) = [\partial\mathcal{V}(\theta)/\partial\theta]_{\theta=\hat{\theta}_m} \in \mathbb{R}^{p \times p}$  based on the log likelihood  $\ell_\theta(\mathcal{D}) = \sum_{i=1}^n \log(f_Y(y_i, x_i))$ . A common stop criterion (as used in `R` (R Core Team, 2021) `glm` function) to determine whether the Fisher scoring has converged or not is when the relative improvement  $|dev_m - dev_{m-1}|/(|dev_m| + 0.1)$  of the deviance  $dev_m = -2 \ln(\ell_{\hat{\theta}_m}(\mathcal{D}))$  is smaller than a value  $a$ . The default value used in the `glm` function of `R` is  $a = 10^{-8}$ .

With non-overlapping data at the  $K$  sites (each subject contributes information only at a unique site), condition (4) is fulfilled. This implies that the additive structure of the global score vector  $\mathcal{V}(\theta_m)$  and Fisher information  $\mathcal{I}(\theta_m)$ . With the site-specific score vector  $\mathcal{V}_k(\theta_m)$  and Fisher information  $\mathcal{I}_k(\theta_m)$ , it holds:

$$\mathcal{V}(\hat{\theta}_m) = \sum_{k=1}^K \mathcal{V}_k(\hat{\theta}_m) \quad (6)$$

$$\mathcal{I}(\hat{\theta}_m) = \sum_{k=1}^K \mathcal{I}_k(\hat{\theta}_m) \quad (7)$$

This process complies with **A1** and allows estimation of the parameter vector  $\hat{\theta}$  with the same precision as in an analysis based on data aggregated over the sites.

#### 4.4 Distributed CIs for the AUC

In Section 4.1, we explain that the distributed calculation of the global sample mean complies with **A1**. We refer to the distributed sample mean calculation as  $\text{distrAVG}(\mathbf{v}^{(1)}, \dots, \mathbf{v}^{(K)})$ . Next, we are interested to calculate a distributed version of the sample variance  $\widehat{\text{var}}(\mathbf{v}) = (n-1)^{-1} \sum_{i=1}^n (v_i - \bar{v})^2$  by a two-step procedure. In the first step, the sample mean is calculated using  $\bar{v} = \text{distrAVG}(\mathbf{v}^{(1)}, \dots, \mathbf{v}^{(K)})$  and shared with all  $K$  sites. In the second step, each site calculates the aggregation  $a_{\text{var}}(\mathbf{v}^{(k)}) = \sum_{i=1}^{n^{(k)}} (v_i^{(k)} - \bar{v})^2$ , which is further aggregated to the sample variance  $\widehat{\text{var}}(\mathbf{v}) = (n-1)^{-1} \sum_{k=1}^K a_{\text{var}}(\mathbf{v}^{(k)})$ . We refer to the distributed sample variance calculation as  $\text{distrVAR}(\mathbf{v}^{(1)}, \dots, \mathbf{v}^{(K)})$ . The operations  $\text{distrAVG}$  and  $\text{distrVAR}$  fulfill **A1** if sufficient observations are present at the single sites:  $n^{(k)} \geq q, \forall k \in \{1, \dots, K\}$ .

The operation  $\text{distrVAR}$  is needed to determine non-disclosing distributed CIs for the global AUC. As shown in Section 3.2 and Section 3.3, the calculation of the approximated CI requires both survivor functions  $\hat{S}_0$  and  $\hat{S}_1$ , which must be approximated by their versions under differential privacy  $\tilde{S}_0$  and  $\tilde{S}_1$  (see Section 4.2). A distributed CI  $\tilde{\text{ci}}_\alpha$  to approximate  $\text{ci}_\alpha$  is calculated using the differential private survivor functions  $\tilde{S}_0$  and  $\tilde{S}_1$  and the variances obtained by  $\text{distrVAR}$ .

## 5 Simulation study

### 5.1 General considerations

It is emphasized in Section 4.3 that the survivor functions for the data at hand are needed to built placement values and to create the data set for the probit regression in order to estimate the ROC curve and its AUC. Based on the Gaussian mechanism, noise is generated to create a non-disclosing distributed survivor function. The aim of the simulation study is to understand the effect of the introduced noise, that is necessary to conduct the distributed analysis, on the accuracy when compared to the empirical AUC and

the CI of DeLong et al. (1988). We assume that the well studied empirical AUC and CI are adequate estimators of the true AUC of the underlying data generating process that are already attached with a certain estimation error. Our goal is not to construct better estimates for the true AUC but to study the difference of our distributed approach to the estimates applied on the pooled data.

In our simulation, we explore the bias introduced by our distributed approach. To assess the accuracy of our distributed approach when estimating the AUC, we measure the difference  $\Delta AUC = AUC - \widetilde{AUC}_{\text{ROC-GLM}}$  of the AUC obtained by the distributed ROC-GLM  $\widetilde{AUC}_{\text{ROC-GLM}}$  (Section 4.1) and the empirical AUC (Section 3.2). Of interest is to have an accuracy of  $|\Delta AUC| \leq 0.01$ .

For the CI, we calculate the error  $\Delta ci_\alpha$  based on the symmetric difference between  $ci_\alpha$  proposed by DeLong et al. (1988, see Section 3.3) and our non-disclosing distributed approach  $\widetilde{ci}_\alpha$  (Section 4.4). We study  $\Delta ci_\alpha = |\widetilde{ci}_{\alpha,l} - ci_{\alpha,l}| + |\widetilde{ci}_{\alpha,r} - ci_{\alpha,r}|$ , with indices  $l$  and  $r$  denote the left and right side of the CI. It is of interest to have an error smaller than 0.01:  $\Delta ci_\alpha < 0.01$ .

We explore the following research questions (RQ):

**RQ1 – Correctness of the ROC-GLM and distributed ROC-GLM** (Section 5.3.1): How to set both privacy parameters  $\varepsilon$  and  $\delta$  to reach  $|\Delta AUC|$  below 0.01?

**RQ2 – Correctness of the AUC CIs** (Section 5.3.2): How to set both privacy parameters  $\varepsilon$  and  $\delta$  to reach  $\Delta ci_\alpha$  below 0.01?

## 5.2 Data generation

(1) The data generation starts with randomly picking  $n$  from  $\{100, \dots, 2500\}$ . (2) For each  $i \in \{1, \dots, n\}$ , the *true* prediction scores are generated from the uniform distribution  $\mathcal{F}_i \sim U[0, 1]$ . Next, (3) the class membership  $y_i \in \{0, 1\}$  is determined by  $y_i = \mathbb{1}(\mathcal{F}_i \geq 0.5)$ . This results in a perfect AUC of 1. (4) The perfect ordering of the class values with respect to individual scores is broken by flipping labels randomly. A set of indexes  $\mathcal{I}$  of size  $\lfloor \gamma n \rfloor$  is selected for which the corresponding labels are replaced by  $y_i \sim \text{Ber}(0.5)$ ,  $\forall i \in \mathcal{I}$ . The fraction  $\gamma$  is sampled from a  $U[0.5; 1]$  distribution. (5) For comparison, the empirical AUC is calculated from the vector of scores  $\mathcal{F}$  and flipped labels  $y$ . (6) The non-disclosing distributed process described in Section 4.1 is used to calculate the  $\widetilde{AUC}_{\text{ROC-GLM}}$  and  $\widetilde{ci}_{0.05}$ . The examined values for the distributed ROC-GLM are described in Section 5.3.1. The simulation is repeated 10000 times.

To demonstrate the effectiveness of the basic non-distributed ROC-GLM AUC estimation, Figure 3 shows the empirical distribution of the empirical as well as ROC-GLM based AUC values depending on the sizes of  $n$ . The distribution of the empirical AUC values is close to the uniform distribution over the range of 0.5 to 1. The behavior of the distribution at the borders can be explained as follows: To obtain an AUC value of one, it is necessary to keep all original class labels  $y$ . However, this happens rarely, due to the randomized assignment of the observations chosen in  $\mathcal{I}$ . The same applies to AUC values close to 0.5. An AUC value of 0.5 appears if the class labels are completely randomized. This is also a rare event.

## 5.3 Results

### 5.3.1 Correctness of the ROC-GLM and distributed ROC-GLM

**ROC-GLM** Figure 3 shows a nearly perfect overlap of the empirical distributions of the empirical as well as basic non-distributed ROC-GLM based AUC values in the range of values between 0.6 and 0.8.

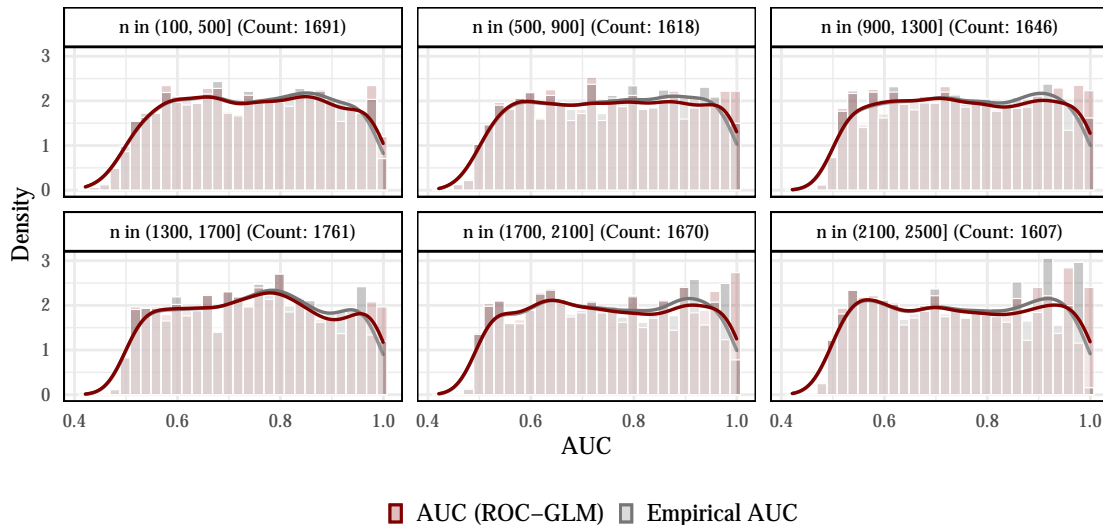


**Figure 3** Densities of 10 000 simulated values of the empirical AUC and AUC from the ROC-GLM. The densities are grouped by different data sizes  $n$ .

Nevertheless, the behavior at the right border results from the fact that the response  $U$  of the probit regression contains only very few values of zero and mostly values of 1 resulting in an unbalanced data situation. This impairs the numerical behavior of the probit regression estimation.

Next, we quantify the difference between the empirical and the basic non-distributed ROC-GLM based AUC estimates:  $(AUC - AUC_{\text{ROC-GLM}})$ . Table 1 shows summary statistics of these differences organized by bins of the empirical AUC of width 0.025. In **RQ1** an absolute difference below 0.01 is requested which is fulfilled over the whole AUC range. The mean and median differences for AUC values ranging from 0.5 to 0.95 fulfill this requirement, whereas AUC values between 0.95 and 0.975 show slightly larger differences.

**Distributed ROC-GLM** In the following, we investigate the accuracy of the AUC estimated by the distributed ROC-GLM. Differential privacy – a necessary component – is determined by the parameters  $\varepsilon$  and  $\delta$ . These parameters must be determined in such a way that **RQ1** holds. The data are distributed over five sites: The simulated prediction scores  $\mathcal{F}$  and true classes  $y$  are randomly split into  $K = 5$  parts  $\mathcal{F}^{(1)}, \dots, \mathcal{F}^{(5)}$  and  $y^{(1)}, \dots, y^{(5)}$ . Our simulation setting uses  $\varepsilon \in A_\varepsilon = \{0.1, 0.2, 0.3, 0.4, 0.5\}$  and  $\delta \in A_\delta = \{0.1, 0.2, 0.3, 0.4, 0.5\}$ . Due to the Gaussian mechanism, we must also take the  $\ell_2$ -sensitivity into account. We assume  $\Delta_2(\hat{f}) \in A_{\Delta_2(\hat{f})} = \{0.01, 0.03, 0.05, 0.07, 0.09\}$ . For the simulation, each setting of the grid  $A_\varepsilon \times A_\delta \times A_{\Delta_2(\hat{f})}$  is evaluated by simulating 10000 data sets (cf. Section 5.2) and hence obtaining 10000  $\widetilde{AUC}_{\text{ROC-GLM}}$  values that are compared to the respective empirical AUC.

Figure 4 shows the simulation results for different  $\varepsilon$  and  $\delta$  combinations. It is checked if the absolute difference of the empirical AUC on the pooled data and the AUC based on the distributed ROC-GLM is below 0.01 or not. The results are based on 10000 simulation runs for 25  $\varepsilon - \delta$ -combinations and for each  $\Delta_2(\hat{f}) \in \{0.01, 0.03, 0.05, 0.07, 0.09\}$ .

Figure 4 reveals that the bias between empirical and distributed AUC depends on the  $\ell_2$ -sensitivity. The smaller the sensitivity and hence the better the model  $\hat{f}$ , less noise is required to ensure privacy. Correspondingly, smaller choices of the privacy parameters can and should be used to ensure privacy.

Emp. AUC (Bin)	Min.	1st Qu.	Median	Mean	3rd Qu.	Max.	Sd.	Count
(0.5, 0.525]	-0.0044	-0.0002	0.0002	0.0003	0.0008	0.0053	0.0009	384
(0.525, 0.55]	-0.0052	0.0000	0.0006	0.0006	0.0011	0.0042	0.0010	490
(0.55, 0.575]	-0.0031	0.0003	0.0009	0.0009	0.0015	0.0052	0.0010	463
(0.575, 0.6]	-0.0018	0.0006	0.0012	0.0012	0.0017	0.0052	0.0010	481
(0.6, 0.625]	-0.0044	0.0009	0.0015	0.0014	0.0020	0.0064	0.0010	485
(0.625, 0.65]	-0.0039	0.0012	0.0017	0.0017	0.0022	0.0069	0.0010	501
(0.65, 0.675]	-0.0031	0.0013	0.0018	0.0018	0.0023	0.0068	0.0011	503
(0.675, 0.7]	-0.0022	0.0012	0.0018	0.0018	0.0023	0.0064	0.0010	465
(0.7, 0.725]	-0.0082	0.0010	0.0016	0.0016	0.0023	0.0070	0.0012	523
(0.725, 0.75]	-0.0031	0.0008	0.0015	0.0014	0.0021	0.0087	0.0012	485
(0.75, 0.775]	-0.0058	0.0004	0.0011	0.0010	0.0018	0.0053	0.0013	501
(0.775, 0.8]	-0.0053	-0.0003	0.0004	0.0005	0.0012	0.0088	0.0015	523
(0.8, 0.825]	-0.0061	-0.0013	-0.0002	-0.0004	0.0005	0.0045	0.0016	476
(0.825, 0.85]	-0.0125	-0.0023	-0.0013	-0.0014	-0.0003	0.0059	0.0019	484
(0.85, 0.875]	-0.0111	-0.0037	-0.0026	-0.0025	-0.0014	0.0074	0.0020	520
(0.875, 0.9]	-0.0136	-0.0056	-0.0044	-0.0043	-0.0030	0.0076	0.0023	534
(0.9, 0.925]	-0.0195	-0.0080	-0.0065	-0.0065	-0.0052	0.0066	0.0026	515
(0.925, 0.95]	-0.0193	-0.0105	-0.0091	-0.0089	-0.0076	0.0056	0.0030	481
(0.95, 0.975]	-0.0227	-0.0138	<b>-0.0113</b>	<b>-0.0113</b>	-0.0093	0.0067	0.0037	503
(0.975, 1]	-0.0180	-0.0093	-0.0062	-0.0064	-0.0034	0.0013	0.0039	529

**Table 1** Minimum, 0.25-quantile/1st quantile, median, mean, 0.75-quantile/3rd quantile, maximum, standard deviation, and the number of values of the differences  $AUC - AUC_{\text{ROC-GLM}}$  of the bins containing the respective subset of the 10000 empirical AUC values. Bold values indicates that these AUC bins do not fulfil **RQ1**.

Based on the results, we choose  $(\varepsilon, \delta) = (0.2, 0.1)$  for  $\Delta_2(\hat{f}) \leq 0.01$ ,  $(\varepsilon, \delta) = (0.3, 0.4)$  for  $\Delta_2(\hat{f}) \in (0.01, 0.03]$ ,  $(\varepsilon, \delta) = (0.5, 0.3)$  for  $\Delta_2(\hat{f}) \in (0.03, 0.05]$ , and  $(\varepsilon, \delta) = (0.5, 0.5)$  for  $\Delta_2(\hat{f}) \in (0.05, 0.07]$ . Based on the simulation, we recommend to use our distributed approach for settings with  $\Delta_2(\hat{f}) > 0.07$  with caution and highlight that the accuracy of the AUC estimator suffers because of too much generated noise.

### 5.3.2 Correctness of the AUC CIs

The respective results in terms of acceptable  $(\varepsilon, \delta)$  combinations are shown in Figure 5. Acceptable  $(\varepsilon, \delta)$  combinations under **RQ1** are also acceptable under **RQ2**. Therefore, we recommend to use the more restrictive settings as described in the previous Section 5.3.1 for the AUC estimation of the distributed ROC-GLM.

## 6 Data analysis

In this chapter we develop a prognostic model and validate its predictive performance on a distributed test data set. The following presents the distributed analysis which is also compared to the pooled analysis (see Section 6.4). As privacy level, we choose a value of  $q = 5$  (see Section 4.1, **A1**).

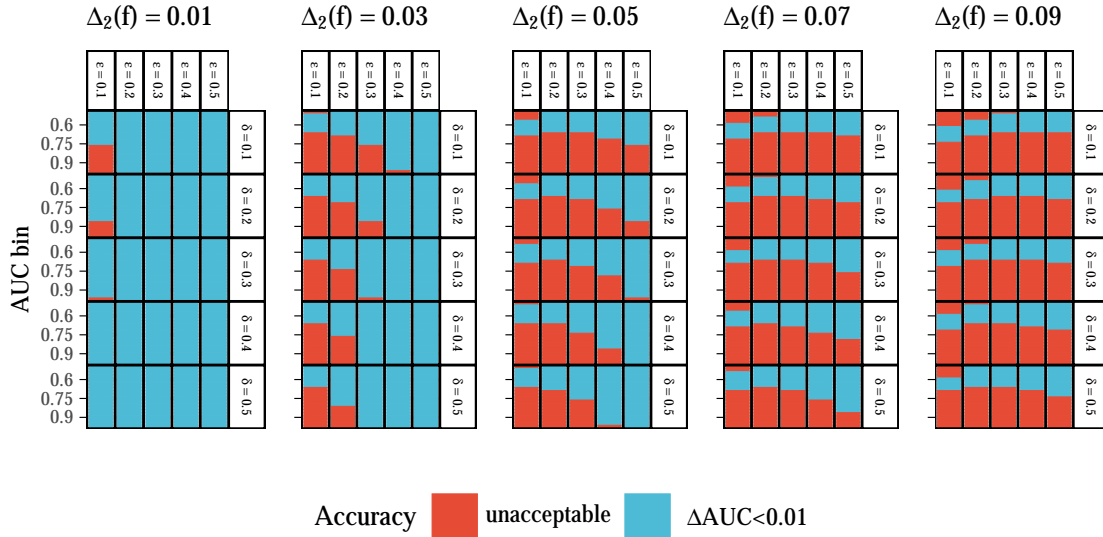


**Figure 4** Combinations of the privacy parameters  $\varepsilon$  and  $\delta$  and their applicability. Each rectangle contains empirical AUC bins of size 0.025 (cf. Table 1) and visualizes the mean of the absolute difference  $|\Delta AUC|$  (mean absolute error, MAE) of the distributed AUC compared to the empirical AUC per bin. Each rectangle corresponds to one simulation setting  $(\Delta_2(\hat{f}), \varepsilon, \delta)$ . The MAE per bin is categorized according to our hypothesis with blue visualizing an MAE  $\leq 0.01$  (**RQ1**) while red shows an unacceptable accuracy measured as MAE bigger than 0.01.

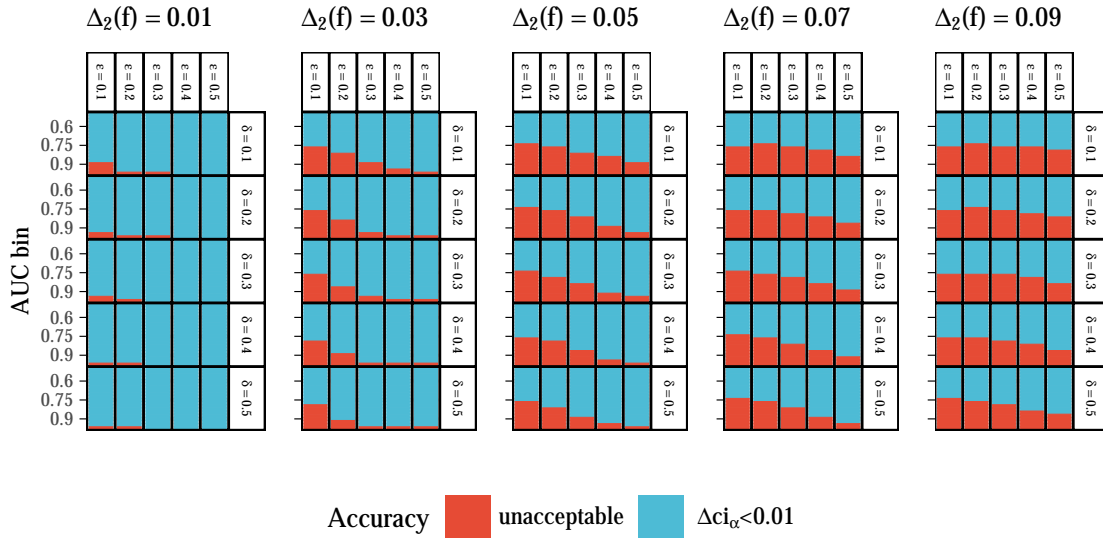


**Figure 5** Combinations of the privacy parameters  $\varepsilon$  and  $\delta$  and their applicability depending on  $\Delta_2(\hat{f})$ . Each rectangle contains empirical AUC bins of size 0.025 (cf. Table 1) and visualizes the mean of the relative error  $\Delta ci_{0.05}$  of the distributed CI  $\tilde{ci}_{0.05}$  compared to  $ci_{0.05}$ . Blue shows accuracy values with  $\Delta ci_{0.05} \leq 0.01$  (**RQ2** applies), while red visualizes inaccuracies of  $\Delta ci > 0.01$ .

**About the data** The data set is provided by the German Breast Cancer Study Group (Schumacher et al., 1994) and can be found in the `TH.data` package (Hothorn, 2021). The data consists of records from 686 breast cancer patients on the effect of hormonal therapy on survival. Besides the binary variable hormonal treatment (`horTh`) the data set provides information on age (`age`), menopausal status (`menostat`), tumor size (in mm, `tsize`), tumor grade (`tgrade`), number of positive nodes (`pnodes`), progesterone receptor (in fmol, `progrec`), estrogen receptor (in fmol, `estrec`), recurrence-free survival time (in days, `time`), and censoring indicator (0- censored, 1- event, `cens`).

Because the data set is (by its nature) not distributed, we use 60 % (412 observations) for training the model and split the remaining 40 % (274 observations) into 5 parts  $\mathcal{D}^{(1)}, \dots, \mathcal{D}^{(5)}$  with  $n^{(1)} = 56$ ,  $n^{(2)} = 49$ ,  $n^{(3)} = 60$ ,  $n^{(4)} = 49$ , and  $n^{(5)} = 60$  that are used for evaluation. Each split is distributed to a site to simulate the distributed setup.

The aim is to predict the survival probability  $p(t|\mathbf{x}) = P(T > t|X = \mathbf{x})$  of surviving time point  $t$  based on covariates  $\mathbf{x}$ . For the use-case, we choose  $t = 730$  (two years) and, therefore, the goal is to validate the survival probability of a patient after two years in the study. The predicted scores are the survival probabilities  $\hat{y}_i = \hat{f}(\mathbf{x}_i) = \hat{p}(730|\mathbf{x}_i)$  with  $\mathbf{x}_i \in \cup_{k=1}^K \mathcal{D}^{(k)}$ . The corresponding binary variable  $y_i$  equals 0 if the patient dies in  $[0, 730]$  or an recurrence was observed and 1 otherwise. Therefore, a high value for the survival probability  $\hat{y}_i$  ideally corresponds to a binary outcome of 1.

**About the model** We choose a random forest (Breiman, 2001) using the R package `ranger` (Wright and Ziegler, 2017) as prognostic model  $\hat{f}$  for the survival probability  $p(t|\mathbf{x})$ . With exception of the number of trees, which is set to 20, the random forest was trained with the default hyperparameter settings of the `ranger` implementation. The model formula is given by

$$\text{Surv}(\text{time}, \text{cens}) \sim \text{horTh} + \text{age} + \text{tsize} + \text{tgrade} + \text{pnodes} + \text{progrec} + \text{estrec}.$$

**About the implementation** The implementation of the methods is based on the DataSHIELD (Gaye et al., 2014) framework and is provided by a collection of packages with each fulfilling a specific task:

- **dsPredictBase** ([github.com/difuture-lmu/dsPredictBase](https://github.com/difuture-lmu/dsPredictBase))
- **dsCalibration** ([github.com/difuture-lmu/dsCalibration](https://github.com/difuture-lmu/dsCalibration))
- **dsROCGLM** ([github.com/difuture-lmu/dsROCGLM](https://github.com/difuture-lmu/dsROCGLM))

Further details about methods and privacy considerations can be found in the respective GitHub README.

**Aim of the analysis** The main goal of the analysis is to test the hypothesis that the true AUC is significantly bigger than 0.6 as minimal prognostic performance of the model  $\hat{f}$ . The significance level is set to  $\alpha = 0.05$ :

$$H_0 : AUC \leq 0.6 \text{ vs. } H_1 : AUC > 0.6 \tag{8}$$

To test the hypothesis, we estimate the AUC with  $\widetilde{AUC}_{\text{ROC-GLM}}$  using the distributed ROC-GLM as well as the approximated CI  $\widetilde{ci}_{0.05}$ . We reject  $H_0$  if  $AUC > 0.6$ ,  $\forall AUC \in \widetilde{ci}_{0.05}$ .

**Analysis plan** In the following, (1) we start in with the calculation of the  $\ell_2$ -sensitivity (Section 6.1). Depending on the result, we set the privacy parameters  $\epsilon$  and  $\delta$ . Next, (2) we continue with fitting the

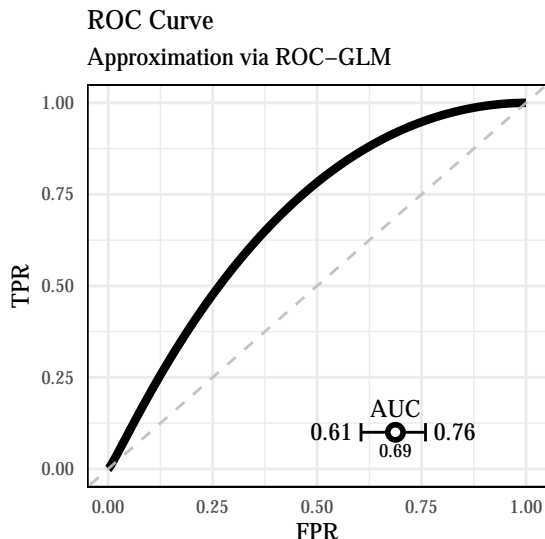


**Figure 6** ROC curve estimated by the distributed ROC-GLM.

distributed ROC-GLM and calculating the approximation of the AUC CI (Section 6.2). At this point, we are able to make a decision about the hypothesis in equation (8). In a final step, (3) we demonstrate how to check the calibration of the model using the distributed Brier score and calibration curve (Section 6.3).

### 6.1 Choice of the privacy parameters

Given the model and the data set, the  $\ell_2$ -sensitivity is  $\Delta_2(\hat{f}) = 0.016$ . Following the results of Section 5.3.1, we use  $\varepsilon = 0.3$  and  $\delta = 0.4$ , as suggested for  $\Delta_2(\hat{f}) \in (0.01, 0.03]$ .

### 6.2 Calculation of the distributed ROC-GLM

The fit of the ROC-GLM results in parameter estimates of  $\gamma_1 = 0.7817$  and  $\gamma_2 = 1.2486$ . The AUC obtained from the ROC curve using these parameters is  $AUC_{\text{ROC-GLM}} = 0.6875$  with  $\tilde{c}_{0.05} = [0.6051, 0.7595]$ . The results are visualized in Figure 6.

Based on the given CI, we significantly reject  $H_0$  for  $H_1$  and hence assume the true AUC to be greater than 0.6.

### 6.3 Checking the calibration

The Brier score of  $\hat{f}$  calculates to  $BS = 0.1733$  and indicates a good but not perfect calibration. We further assume our model to be not calibrated perfectly. Still, the calibration is adequate but the model seems to underestimate the true relative frequencies for scores greater than 0.3. Figure 7 shows the distributed calibration curve as well as the individual calibration curves per site. Furthermore, we observe that the range of the calibration curve does not cover the whole range of the scores  $\hat{f}(x) \in [0, 1]$ . This indicates that our model is not predicting scores close to 1. We want to highlight that due to privacy reasons not all score values were included into the calculation. Aggregated values are just shared if they consist out of at least 5 elements. The table in Appendix A.3 shows the amount of elements per bin and site.

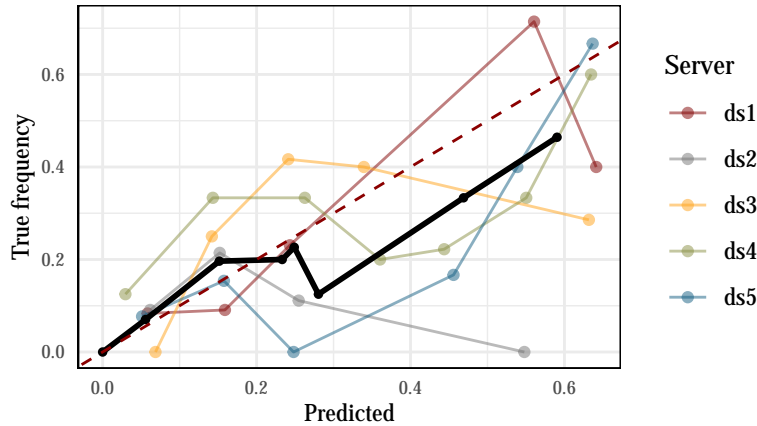


**Figure 7** Calibration curve (bold line) and calibration curves of the individual sites using 10 bins. Note that aggregated values from the site are only shared if one bin contains more than 5 values. See Appendix A.3 for tables containing the numbers of values per bin.

#### 6.4 Comparison with pooled data

Comparing the ROC curves using the empirical ROC and the distributed ROC-GLM (Figure 8, left) shows a good fit of the ROC-GLM. The resulting AUC values are  $\widetilde{AUC}_{\text{ROC-GLM}} = 0.6875$  and  $AUC = 0.6919$  with  $|\Delta AUC| = 0.0044 < 0.01$ . The CIs of the approximated CI  $\widetilde{ci}_{0.05} = [0.6051, 0.7595]$  and the CI on the pooled scores  $ci_{0.05} = [0.6131, 0.7608]$  reveals a slightly more pessimistic CI estimation in the distributed setup. The error of the CI calculates to  $\Delta ci_{0.05} = 0.0094 < 0.01$ .

The distributed calibration curve shows a good overlap with the calibration curve in areas, where all data are allowed to get shared. For bins where this is not the case, the distributed calibration curve is off. Still the tendency of over or underestimation of the distributed calibration curve corresponds to the one of the pooled curve. The bins for which the full information was received are  $[0, 0.1]$ ,  $(0.1, 0.2]$ , and  $(0.2, 0.3]$  (cf. Appendix A.3 table 2). For all other bins, at least one site was not allowed to share the aggregated values. The Brier score of the pooled and distributed approach is equal.

## 7 Reproducibility considerations

All experiments were conducted using R version 4.1.2 on a Linux machine with an Intel(R) Core(TM) i7-8665U CPU @ 1.90GHz processor. The package used to run the simulation was `batchtools` (Lang et al., 2017). The code to reproduce all results as well as all simulation results is available in a GitHub repository<sup>2</sup>. The repository contains a README file with further details and a script to install all packages with the respective version used when the benchmark was conducted. Furthermore, a Docker image<sup>3</sup> can be installed providing a snapshot of the system at the time of the benchmark containing R and all packages with their respective version. The Docker image also comes with the RStudio container<sup>4</sup> that allows to directly inspect all the results in a web browser.

<sup>2</sup> [github.com/difuture-lmu/simulations-distr-auc](https://github.com/difuture-lmu/simulations-distr-auc)

<sup>3</sup> [hub.docker.com/repository/docker/schalkdaniel/simulations-distr-auc](https://hub.docker.com/repository/docker/schalkdaniel/simulations-distr-auc)

<sup>4</sup> [hub.docker.com/r/rocker/rstudio](https://hub.docker.com/r/rocker/rstudio)



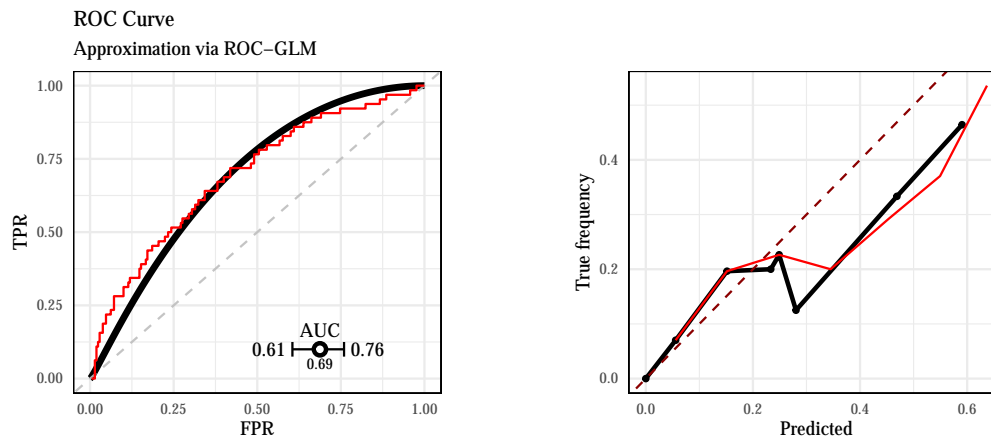


**Figure 8** Comparison of the empirical ROC curve with ROC curve obtained by the distributed ROC-GLM (left). Comparison of the calibration curve when calculated on the pooled scores compared with the distributed calibration curve (right). The thin curves are the lines on the pooled data.

The code to conduct the data analysis is given in a separate GitHub repository<sup>5</sup>. The repository contains the data, an installation of all necessary packages, as well as code to setup the publicly available DataSHIELD server<sup>6</sup> to run the analysis<sup>7</sup>.

## 8 Discussion

Distributed non-disclosing (i.e., privacy-preserving) strategies for data analysis are highly relevant for data-driven biomedical research. Since the analyses can be considered as anonymous, current legal data protection frameworks allow their use without requesting specific consent. The protection of privacy by appropriate means is fundamental when using personal data for research. These technologies also enable taking part in broader network structures without additional administrative work concerning data protection issues. Privacy-preserving distributed computation allows researchers to digitally cooperate and leverage the value of their data while respecting data sovereignty and without compromising privacy.

Wide international activity has been dedicated to setting up distributed non-disclosing analysis frameworks, which implement machine learning approaches into a distributed analysis scheme. The availability of the respective algorithms is growing, and distributed learning for data from heterogeneous clinical servers has emerged as a hot field. However, it is our impression that algorithms for distributed validation of these learning algorithms are lacking.

In this paper, we specifically focused on the assessment of discrimination and calibration of learning algorithms with a binary outcome. The discrimination is estimated by a ROC curve and its AUC. We also provide CIs to the distributed AUC estimate. The distributed estimation process is based on *placement values* and *survivor functions*. They represent qualities of the global distribution of score values (aggregated

<sup>5</sup> [github.com/difuture-lmu/datashield-roc-glm-demo](https://github.com/difuture-lmu/datashield-roc-glm-demo)

<sup>6</sup> Available at [opal-demo.obiba.org](https://opal-demo.obiba.org), the reference, username, and password are available at the OPAL documentation [opaldoc.obiba.org/en/latest/resources.html](https://opaldoc.obiba.org/en/latest/resources.html) in the “Types” section.

<sup>7</sup> We cannot guarantee the functionality of the DataSHIELD server and if it will be publicly available forever. However, we keep the repository up-to-date by using continuous integration, which is triggered automatically every week. This system also reports errors that occur if the analysis cannot be conducted on the test server anymore. Further information can be found in the README file of the repository.

over all centers). To do this in a non-disclosing way, we applied techniques of differential privacy. With the creation of the placement values and the transmission of this information to the local server, we applied a distributed version of the ROC-GLM approach to estimate the ROC curve and its AUC in a distributed way. We used a straightforward approach for the distributed GLM estimation. However, we acknowledge that there may be more efficient approaches, and we will explore this aspect in future work.

We implemented an algorithm with R to be used within DataSHIELD. We have demonstrated its applicability to real-world data.

### Conflict of Interest

*The authors have declared no conflict of interest.*

### Acknowledgments

*This work was supported by the German Federal Ministry of Education and Research (BMBF) under Grant No. 01IS18036A and Federal Ministry for Research and Technology (BMFT) under Grant No. 01ZZ1804C (DIFUTURE, MII). The authors of this work take full responsibilities for its content.*

## Appendix

### A.1. Decomposition of score vector and Fisher information

$$\begin{aligned} \mathcal{V}(\hat{\theta}_m) &= \left[ \frac{\partial \ell_\theta(\mathcal{D})}{\partial \theta} \right]_{\theta=\hat{\theta}_m} = \left[ \frac{\partial \sum_{i=1}^n \log(f_Y(y_i, x_i))}{\partial \theta} \right]_{\theta=\hat{\theta}_m} \\ &= \left[ \sum_{i=1}^n \frac{\partial \log(f_Y(y_i, x_i))}{\partial \theta} \right]_{\theta=\hat{\theta}_m} = \sum_{k=1}^K \left[ \sum_{(y,x) \in \mathcal{D}^{(k)}} \frac{\partial \log(f_Y(y, x))}{\partial \theta} \right]_{\theta=\hat{\theta}_m} \\ &= \sum_{k=1}^K \left[ \frac{\partial \log(\ell_\theta(\mathcal{D}^{(k)}))}{\partial \theta} \right]_{\theta=\hat{\theta}_m} = \sum_{k=1}^K \mathcal{V}_k(\hat{\theta}_m) \end{aligned}$$

$$\begin{aligned} \mathcal{I}(\hat{\theta}_m) &= \left[ \frac{\partial \mathcal{V}(\theta)}{\partial \theta} \right]_{\theta=\hat{\theta}_m} = \left[ \frac{\partial \sum_{k=1}^K \mathcal{V}_k(\hat{\theta}_m)}{\partial \theta} \right]_{\theta=\hat{\theta}_m} = \\ &= \sum_{k=1}^K \left[ \frac{\partial \mathcal{V}_k(\hat{\theta}_m)}{\partial \theta} \right]_{\theta=\hat{\theta}_m} = \sum_{k=1}^K \mathcal{I}_k(\hat{\theta}_m) \end{aligned}$$

### A.2. Illustration of the gaussian mechanism

The noise  $r$  added in the Gaussian mechanism to obtain a noise representation of scores  $\hat{f}(x)$  highly depends on the three values of  $\Delta_2(f)$ ,  $\varepsilon$ , and  $\delta$ . In our approach, we first look at the value of  $\Delta_2(f)$  and then set  $\varepsilon$  and  $\delta$  accordingly to not introduce too much noise and hence worsen the accuracy. Figure 9 and Figure 10 visualizes the Gaussian mechanism for  $\Delta_2(f) \in \{0.01, 0.05\}$ ,  $\varepsilon \in \{0.1, 0.3, 0.5\}$  and  $\delta \in \{0.1, 0.3, 0.5\}$  to get an idea of how the noise distorts the score values  $f(x)$ . The figures contain the score values (upper labels), the value of the variance  $\tau^2$  (which is based on  $\Delta_2(f)$ ,  $\varepsilon$ , and  $\delta$ ), the respective density of the normal distribution, and the noisy score values (lower labels). It also visualizes how the Gaussian mechanism changes the order of the scores depending on the noise.

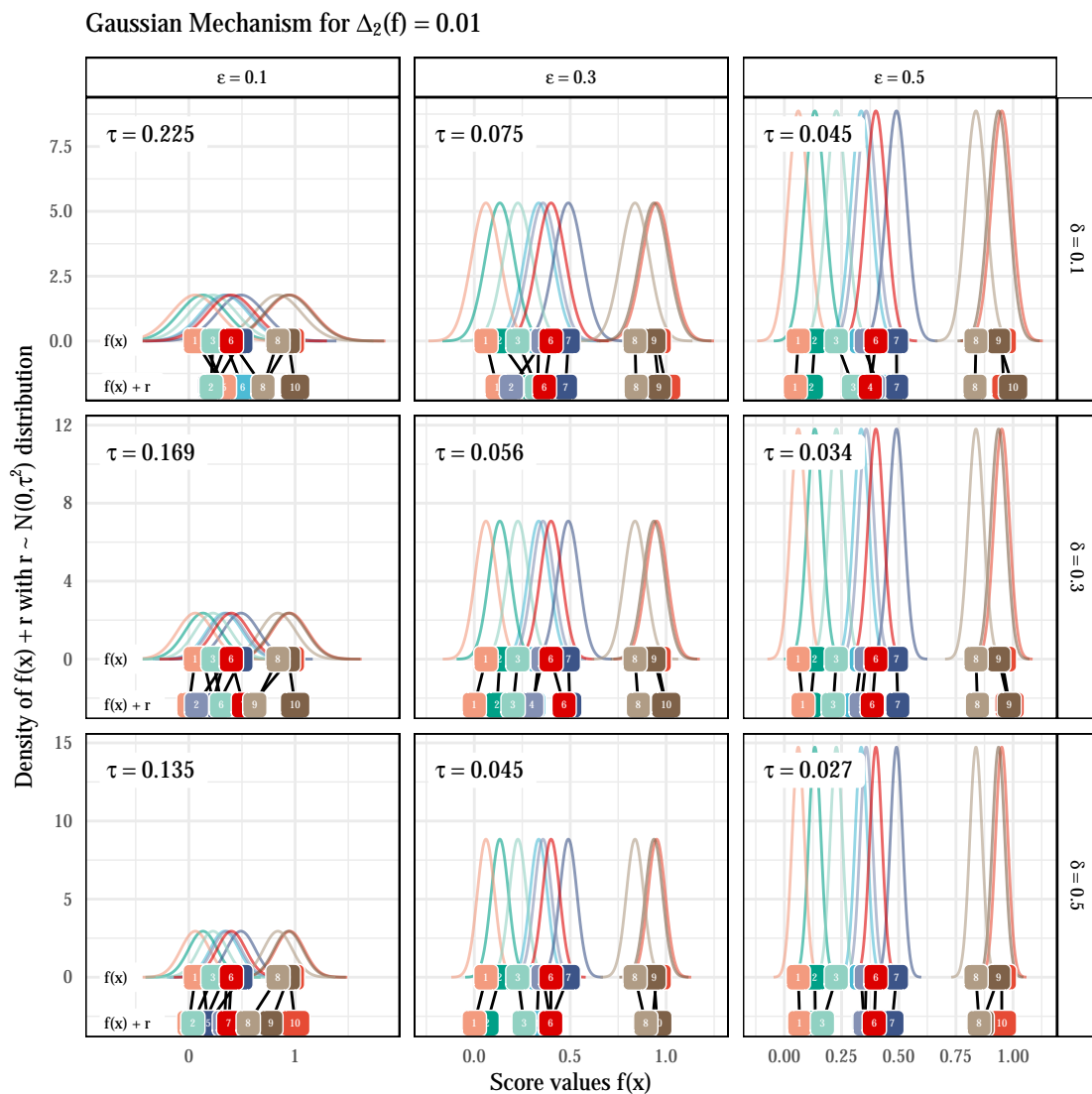


**Figure 9** Visualization how the Gaussian mechanism adds noise to the original score values  $f(x)$  (upper labels) to get a noisy representation  $f(x) + r$  (lower labels) with  $r \sim \mathcal{N}(0, \tau^2)$ . At each point  $f(x)$  the corresponding density of  $\mathcal{N}(f(x), \tau^2)$  is added to visualize how the Gaussian mechanism shuffles the order (lines between the two labels of  $f(x)$  and  $f(x) + r$ ) of the score values depending on the variance  $\tau^2$ . The whole mechanism depends on the  $\ell_2$ -sensitivity which is set to 0.01 here.

### A.3. Number of observations per bin for the calibration curves

#### References

- Arellano, A. M., Dai, W., Wang, S., Jiang, X., and Ohno-Machado, L. (2018). Privacy policy and technology in biomedical data science. *Annual review of biomedical data science*, 1:115–129.
- Boyd, K., Lantz, E., and Page, D. (2015). Differential privacy for classifier evaluation. In *Proceedings of the 8th ACM Workshop on Artificial Intelligence and Security*, pages 15–23.

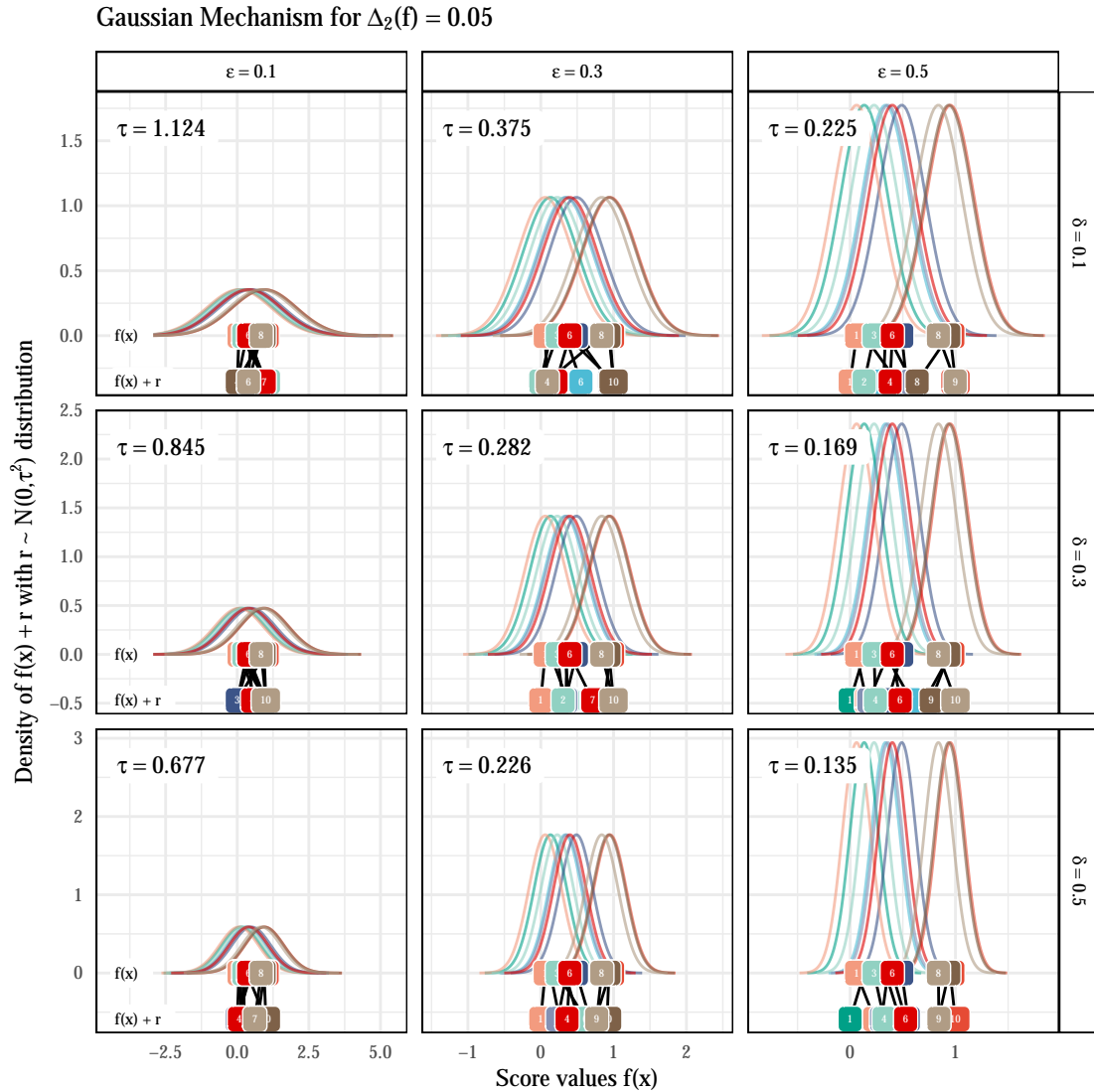


**Figure 10** Visualization how the Gaussian mechanism adds noise to the original score values  $f(x)$  (upper labels) to get a noisy representation  $f(x) + r$  (lower labels) with  $r \sim \mathcal{N}(0, \tau^2)$ . At each point  $f(x)$  the corresponding density of  $\mathcal{N}(f(x), \tau^2)$  is added to visualize how the Gaussian mechanism shuffles the order (lines between the two labels of  $f(x)$  and  $f(x) + r$ ) of the score values depending on the variance  $\tau^2$ . The whole mechanism depends on the  $\ell_2$ -sensitivity which is set to 0.05 here.

Breiman, L. (2001). Random forests. *Machine learning*, 45(1):5–32.

Brier, G. W. et al. (1950). Verification of forecasts expressed in terms of probability. *Monthly weather review*, 78(1):1–3.

DeLong, E. R., DeLong, D. M., and Clarke-Pearson, D. L. (1988). Comparing the areas under two or more correlated receiver operating characteristic curves: a nonparametric approach. *Biometrics*, pages 837–845.

Duan, R., Boland, M. R., Liu, Z., Liu, Y., Chang, H. H., Xu, H., Chu, H., Schmid, C. H., Forrest, C. B., Holmes, J. H., et al. (2020). Learning from electronic health records across multiple sites: A communication-efficient and

Site k	Bin									
	(0, .1]	(.1, .2]	(.2, .3]	(.3, .4]	(.4, .5]	(.5, .6]	(.6, .7]	(.7, .8]	(.8, .9]	(0.9, 1]
1	<b>12</b>	<b>11</b>	<b>13</b>	3	2	<b>7</b>	<b>5</b>	0	0	0
2	<b>11</b>	<b>14</b>	<b>9</b>	1	4	<b>5</b>	2	0	0	0
3	<b>13</b>	<b>12</b>	<b>12</b>	<b>5</b>	3	4	<b>7</b>	1	0	0
4	<b>8</b>	<b>6</b>	<b>9</b>	<b>5</b>	<b>9</b>	<b>6</b>	<b>5</b>	0	0	0
5	<b>13</b>	<b>13</b>	<b>10</b>	1	<b>6</b>	<b>5</b>	<b>9</b>	1	0	0
$\Sigma$	<b>57</b>	<b>56</b>	<b>53</b>	<b>15</b>	<b>24</b>	<b>27</b>	<b>28</b>	2	0	0

**Table 2** Number of observations per bin. Values in these bins are just shared if the numbers per bin are bigger than 5. The values for which this applies are highlighted as bold numbers.

- privacy-preserving distributed algorithm. *Journal of the American Medical Informatics Association*, 27(3):376–385.
- Dwork, C. (2006). Differential privacy. In *International Colloquium on Automata, Languages, and Programming*, pages 1–12. Springer.
- Dwork, C., Kenthapadi, K., McSherry, F., Mironov, I., and Naor, M. (2006a). Our data, ourselves: Privacy via distributed noise generation. In *Annual International Conference on the Theory and Applications of Cryptographic Techniques*, pages 486–503. Springer.
- Dwork, C., McSherry, F., Nissim, K., and Smith, A. (2006b). Calibrating noise to sensitivity in private data analysis. In *Theory of cryptography conference*, pages 265–284. Springer.
- Dwork, C., Roth, A., et al. (2014). The algorithmic foundations of differential privacy. *Found. Trends Theor. Comput. Sci.*, 9(3-4):211–407.
- Gaye, A., Marcon, Y., Isaeva, J., LaFlamme, P., Turner, A., Jones, E. M., Minion, J., Boyd, A. W., Newby, C. J., Nuotio, M.-L., et al. (2014). Datashield: taking the analysis to the data, not the data to the analysis. *International journal of epidemiology*, 43(6):1929–1944.
- Hothorn, T. (2021). *TH.data: TH's Data Archive*. R package version 1.1-0.
- Jones, E. M., Sheehan, N. A., Gaye, A., Laflamme, P., and Burton, P. (2013). Combined analysis of correlated data when data cannot be pooled. *Stat*, 2(1):72–85.
- Lang, M., Bischl, B., and Surmann, D. (2017). batchtools: Tools for r to work on batch systems. *The Journal of Open Source Software*, 2(10).
- Loukides, G., Denny, J. C., and Malin, B. (2010). The disclosure of diagnosis codes can breach research participants' privacy. *Journal of the American Medical Informatics Association*, 17(3):322–327.
- Lu, C.-L., Wang, S., Ji, Z., Wu, Y., Xiong, L., Jiang, X., and Ohno-Machado, L. (2015). Webdisco: a web service for distributed cox model learning without patient-level data sharing. *Journal of the American Medical Informatics Association*, 22(6):1212–1219.
- McMahan, B., Moore, E., Ramage, D., Hampson, S., and y Arcas, B. A. (2017). Communication-efficient learning of deep networks from decentralized data. In *Artificial intelligence and statistics*, pages 1273–1282. PMLR.
- Pepe, M. S. (2000). An interpretation for the roc curve and inference using glm procedures. *Biometrics*, 56(2):352–359.
- Pepe, M. S. (2003). The Statistical Evaluation of Medical Tests for Classification and Prediction. *Journal of the American Statistical Association*.
- Piessens, R., de Doncker-Kapenga, E., Überhuber, C. W., and Kahaner, D. K. (2012). *Quadpack: a subroutine package for automatic integration*, volume 1. Springer Science & Business Media.
- Prasser, F., Kohlbacher, O., Mansmann, U., Bauer, B., and Kuhn, K. A. (2018). Data integration for future medicine (difuture). *Methods Inf Med*, 57(S01):e57–e65.
- R Core Team (2021). *R: A Language and Environment for Statistical Computing*. R Foundation for Statistical Computing, Vienna, Austria.
- Schumacher, M., Bastert, G., Bojar, H., Hübner, K., Olschewski, M., Sauerbrei, W., Schmoor, C., Beyerle, C., Neumann, R., and Rauschecker, H. (1994). Randomized 2 x 2 trial evaluating hormonal treatment and the duration of chemotherapy in node-positive breast cancer patients. german breast cancer study group. *Journal of Clinical*

- Oncology*, 12(10):2086–2093.
- Ünal, A. B., Pfeifer, N., and Akgün, M. (2021). ppaurora: Privacy preserving area under receiver operating characteristic and precision-recall curves with secure 3-party computation. *ArXiv*, 2102.
- Van Calster, B., McLernon, D. J., Van Smeden, M., Wynants, L., and Steyerberg, E. W. (2019). Calibration: the achilles heel of predictive analytics. *BMC medicine*, 17(1):1–7.
- Vuk, M. and Curk, T. (2006). Roc curve, lift chart and calibration plot. *Metodoloski zvezki*, 3(1):89.
- Wright, M. N. and Ziegler, A. (2017). ranger: A fast implementation of random forests for high dimensional data in C++ and R. *Journal of Statistical Software*, 77(1):1–17.
- Wu, Y., Jiang, X., Kim, J., and Ohno-Machado, L. (2012). Grid binary logistic regression (glore): building shared models without sharing data. *Journal of the American Medical Informatics Association*, 19(5):758–764.
- Yang, C., Wang, Q., Xu, M., Chen, Z., Bian, K., Liu, Y., and Liu, X. (2021). Characterizing impacts of heterogeneity in federated learning upon large-scale smartphone data. In *Proceedings of the Web Conference 2021*, pages 935–946.
- Zweig, M. H. and Campbell, G. (1993). Receiver-operating characteristic (roc) plots: a fundamental evaluation tool in clinical medicine. *Clinical chemistry*, 39(4):561–577.